ARTICLE
Journal of Cellular Biochemistry 108:476–488 (2009)

Journal of Cellular Biochemistry

Distribution of TGF-β Isoforms and Signaling Intermediates in Corneal Fibrotic Wound Repair

Man-IL Huh,[1] Yeoun-Hee Kim,[1] Jong-Hyuck Park,[1] Sung-Won Bae,[1] Min-Hee Kim,[1] Yongmin Chang,[2] Song-Ja Kim,[3] Sun-Ryung Lee,[4] Young-Sup Lee,[5] Eun-Jung Jin,[6] Jong-Kyung Sonn,[1] Shin-Sung Kang,[1] and Jae-Chang Jung[1*]

[1]*Department of Biology, College of Natural Sciences, Kyungpook National University, Daegu 702-701, South Korea*

[2]*Department of Diagnostic Radiology, College of Medicine, Kyungpook National University, Daegu 702-422, South Korea*

[3]*Department of Life Science, Kongju National University, Kongju 314-701, South Korea*

[4]*Department of Life Science, Cheju National University, Jeju 690-756, South Korea*

[5]*Department of Biochemistry, College of Natural Sciences, Kyungpook National University, Daegu 702-701, South Korea*

[6]*Division of Biological Science, College of Natural Sciences, Wonkwang University, Iksan, South Korea*

ABSTRACT

In this study, temporal and spatial distribution of three TGF-β isoforms and their downstream signaling pathways including pSmad2 and p38MAPK were examined during fibrotic wound repair. In normal chick corneas, TGF-β1, -2, and -3 were weakly detected in Bowman's layer (BL). In healing corneas, TGF-β1 was primarily deposited in the fibrin clot and the unwounded BL. TGF-β2 was highly expressed in healing epithelial and endothelial cells, and numerous active fibroblasts/myofibroblasts. TGF-β3 was mainly detected in the unwound region of basal epithelial cells. α-Smooth muscle actin (α-SMA) was initially appeared in the posterior region of repairing stroma at day 3, and was detected in the entire healing stroma by day 7. Notably, α-SMA was absent in the central region of healing stroma by day 14, and its staining pattern was similar to those of TGF-β2 and p38MAPK. By contrast, pSmad2 was mainly detected in the fibroblasts. In normal cornea, laminin was mainly detected in both epithelial basement membrane (BM) and Descemet's membrane (DM). By contrast to reconstitution of the BM in the wound region, the DM was not repaired although endothelial layer was regenerated, indicating that high levels of TGF-β2 were released into the posterior region of healing stroma on day 14. High levels of α-SMA staining, shown in cultured repair stromal cells from healing corneas on day 14 and in TGF-β2 treated normal stromal cells, were significantly reduced by p38MAPK inhibition. Collectively, this study suggests that TGF-β2-mediated myofibroblast transformation is mediated, at least partly, by the p38MAPK pathway in vivo. J. Cell. Biochem. 108: 476–488, 2009.

KEY WORDS: CORNEAL WOUND HEALING; TGF-β; pSmad2; p38MAPK; FIBROSIS; α-SMA

The fibrotic response is essential for normal wound repair. In the cornea, fibrosis creates opacity, which interferes with vision. Contraction of fibrotic tissue additionally alters corneal shape and the capacity to focus light on the retina. The penetrating wound model is a useful system for studying the basic regulation of fibrotic wound repair [Fini and Stramer, 2005]. Stromal keratocytes are the major cell type contributing to fibrosis in the cornea. Upon ablation wounding, quiescent stromal cells (keratocytes) adjacent to the wound region begin to undergo mitosis along with morphological and functional changes, transform into active fibroblasts, and migrate into the damaged acellular area filled with fibrin clot containing fibronectin and fibrin [Fini and Stramer, 2005]. These active fibroblasts synthesize new extracellular matrix (ECM) molecules distinct from normal uninjured stroma [Fini, 1999]. Once activated by growth factors and cytokines, fibroblasts participate in a number of autocrine and paracrine pathways that

Abbreviations used: TGF-β, transforming growth factor-β; BL, Bowman's layer; α-SMA, α-smooth muscle actin.

Grant sponsor: Korea Research Foundation; Grant numbers: KRF-2006-521-C00148, KRF-2008-521-C00214.

*Correspondence to: Dr. Jae-Chang Jung, PhD, Developmental Biology Laboratory, Department of Biology, College of Natural Sciences, Kyungpook National University, Daegu 702-701, South Korea. E-mail: jcjung@mail.knu.ac.kr

Received 23 April 2009; Accepted 16 June 2009 • DOI 10.1002/jcb.22277 • © 2009 Wiley-Liss, Inc.
Published online 22 July 2009 in Wiley InterScience (www.interscience.wiley.com).

maintain their activation [Wilson et al., 1992; Beales et al., 1999; Lee et al., 2002]. During the contraction phase of wound healing, fibroblasts transform into myofibroblasts expressing α-smooth muscle actin (α-SMA) that imparts contractile properties to cells [Jester et al., 1996; Stramer et al., 2003]. Myofibroblasts also generate abundant ECM which has a composition different from that of the normal, uninjured stroma [Fini and Stramer, 2005]. The altered composition of the ECM synthesized by the myofibroblasts, as well as the disorganized manner of its deposition, probably both contribute the opacity of the fibrotic cornea [Fini and Stramer, 2005]. The ECM of the fibrotic cornea is progressively remodeled over many months by continual synthesis, degradation, and re-synthesis of collagens and other ECM components, which interferes with vision [Girard et al., 1993].

A variety of cytokines and growth factors are involved in corneal wound healing, and their concerted expression and balance, as well as cross-talk between signal transduction pathways are required during wound healing [Wilson et al., 1994; Kim et al., 1999; Derynck and Zhang, 2003; Sharma et al., 2003]. TGF-β is a crucial regulator of corneal wound healing [Jester et al., 1996; Andresen et al., 1997; Myers et al., 1997; Andresen and Ehlers, 1998; Moller-Pedersen et al., 1998; Beales et al., 1999]. The TGF-β superfamily of secreted polypeptides regulates cell proliferation, differentiation, motility, and apoptosis in a variety of cell types. Three isoforms have been identified in mammals to date, designated TGF-β1, -β2, and -β3 [Cheifetz et al., 1990]. Despite structural and functional similarities, the three isoforms differ significantly in terms of potency as growth inhibitors, recognition by receptors, and inactivation by extracellular factors [Cheifetz et al., 1990]. Furthermore, temporal and spatial expression patterns of each TGF-β isoform are discrete in several tissues [Massague, 2003], suggesting that these proteins are physiologically important, and play distinct roles during embryogenesis and adult tissue repair [Cheifetz et al., 1990]. TGF-β triggers an altered fibroblast phenotype typical of wound healing, both in vivo and in vitro [Stramer et al., 2003]. The growth factor additionally stimulates ECM expression and deposition into the pericellular matrix, and controls tissue repair and deregulation of ECM remodeling for corneal fibrosis [Stramer et al., 2003].

Generally, TGF-β is deposited within the extracellular milieu in its latent form, and is not activated except in response to tissue injury that also stimulates its synthesis and release [Barcellos-Hoff, 1996; Koli et al., 2001]. Activation of TGF-β is the key event in initiating and mediating response to tissue damage and tissue repair in vivo. Active TGF-β binds to TGF-β receptor type II (TβR-II), followed by TGF-β receptor type I (TβR-I). In response to receptor activation, Smad2 and Smad3 proteins phosphorylated by TβR-I form heteromeric complexes with Smad4 in the cytoplasm. These complexes translocate to the nucleus to activate transcription of a select set of target genes. Although three principal Smad proteins are involved in mediating the effects of TGF-β, Smad2 and Smad4 are clearly associated with corneal epithelial repair [Hutcheon et al., 2005]. It has been shown that Smad2 and Smad3 have different downstream targets [Piek et al., 2001]. Myofibroblast transformation in repairing corneal wounds is reduced in mice lacking Smad3 [Fini and Stramer, 2005]. In addition, Smad2 knockout in mice results in embryonic lethality [Nomura and Li, 1998; Weinstein et al., 1998]. Importantly, TGF-β activates p38MAPK signaling pathways that influence collagen expression [Tsukada et al., 2005]. Both Smad and p38MAPK signaling pathways mediated by TGF-β are involved in regenerative corneal wound healing and liver fibrosis [Saika, 2004; Tsukada et al., 2005]. However, the relative contributions of Smad2 and p38MAPK signaling pathways in regulating corneal fibrosis remain unclear to date.

The goals of this manuscript were to analyze the distribution of three TGF-β isoforms and some of their signaling pathways, including pSmad2 and p38MAPK, in fibrotic corneal wounds. The employment of these corneal wound models in the chicken is novel and important given that the chicken has a BL like humans, whereas the other commonly used models such as the mouse do not. Here we report that that both pSmad2 and p38MAPK was temporally and spatially regulated during the dynamic processes of fibrotic wound healing through TGF-βs stimulation.

MATERIALS AND METHODS

PENETRATING WOUND PROCEDURES AND EMBEDDING

Surgical procedures were performed in accordance with the ARVO Statement for the Use of Animals in Ophthalmic and Vision Research. A previously characterized mouse and rabbit full-thickness penetrating keratectomy model was adapted to chicks in order to analyze fibrotic repair [Cintron et al., 1973, 1982; Fini and Stramer, 2005]. Two-month-old chicks were anesthetized with an intramuscular injection of ketamine (25 mg/kg) and xylazine (10 mg/kg) before wound creation. Briefly, a 1.0 mm full-thickness button of central corneal tissue demarcated with a trephine was ablated using micro-dissecting scissors. Corneal wounds were allowed to heal for 1, 3, 7, and 14 days. Ten corneas were used for each time-point. At the appropriate times, chicks were sacrificed with an overdose of ketamine and xylazine. Whole corneas were carefully dissected out, and fixed in 4% paraformaldehyde at 4°C overnight. Corneas were dehydrated and trimmed, leaving some normal tissue around the healing wound, cleared with xylene, and embedded in paraffin. Sections (6 μm) were prepared, and maintained until use.

ANTIBODIES AND REAGENTS

Polyclonal antibodies against TGF-β1, TGF-β2, TGF-β3, and p38MAPK were obtained from Santa Cruz Biotechnology (Santa Cruz, CA). Polyclonal pSmad2 antibody was from Cell signaling Technology (Danvers, MA). The SB431542 and monoclonal antibody against α-SMA were purchased from Sigma (St. Louis, MO). The SB203580 was purchased from Calbiochem (San Diego, CA). The monoclonal laminin and fibronectin antibodies were from Developmental studies Hybridoma Bank (University of Iowa, Iowa City, IA). Alexa-Fluor 488-conjugated goat anti-mouse or rabbit IgG and rhodamine-conjugated phalloidin were acquired from Molecular Probes (Eugene, OR). Proteinase K, propidium iodide (PI), and DAPI were purchased from Boehringer Mannheim (Mannheim, Germany) and Vector Laboratories (Burlingame, CA).

IMMUNOHISTOCHEMISTRY

Slides containing paraffin sections were deparaffinized in xylene, and subsequently rehydrated through ethanol series. Sections were rinsed in 0.1 M Tris-buffered saline (TBS; pH 7.4), and permeabilized with 0.3% Triton X-100 in TBS at room temperature for 10 min. To block non-specific binding, sections were incubated with blocking solution (5% normal goat serum and bovine serum albumin in TBS) at room temperature for 1 h, and subsequently processed for indirect immunofluorescence localization using antibodies against TGF-β1, TGF-β2, TGF-β3, α-SMA, p38MAPK, and pSmad2. For the negative control, primary antibodies were omitted, and incubation was performed with 5% normal goat serum. To detect laminin, sections were digested at 37°C with proteinase K (100 μg/ml) for 5 min before primary antibody incubation. Next, sections were washed with TBS, and incubated with the corresponding secondary antibodies conjugated with Alexa-Fluor 488 at room temperature for 1 h. Prior to mounting, slides were washed three times with TBS, and all sections were counterstained with propidium iodide (PI; 10 μg/ml) for nuclear staining. Digital images were captured on a laser scanning confocal image system (MRC-1000; Bio-Rad).

STROMAL CELLS CULTURE AND IMMUNOFLUORESCENCE STAINING

Fourteen days after wound healing, five animals were euthanized by lethal injection with sodium pentobarbital, and the corneas removed. The repair tissue occupying the original penetrating wound was isolated. Uninjured three normal chick corneas were also removed. Corneal stromal cells were isolated and cultured, as described previously [Jung et al., 2007]. Second passages of repair or normal stromal cells were seeded at 1.5×10^4 cells per eight-chamber slide (Tissue-Tek; VWR Scientific) in F-12 medium containing 10% FCS, and allowed to attach and spread overnight, and the medium was replaced with a serum-free medium and cells were cultured for 24 h. To determine whether α-SMA expression is regulated TGF-β2, cells were treated with TGF-β2 (2 ng/ml) in serum free medium, either together with SB203580 (20 μM) as inhibitor of p38MAPK or SB431542 (20 μM) as inhibitor of TGF-β type I receptor kinase for 24 h. For co-visualizing α-SMA and actin filaments, the medium was removed, and the cell layer washed twice with PBS and fixed with 4% paraformaldehyde in PBS for 5 min. Cells were permeabilized in 0.3% Triton X-100 for 2 min, and incubated with a FITC-conjugated monoclonal α-SMA antibody and TRITC-conjugated phalloidin at RT for 1 h. Nuclei were visualized by staining with DAPI. Prior to mounting, cells were washed three times with PBS. Images were captured on a Zeiss fluorescence microscope.

The percentage of myofibroblasts from the cultured stromal cells was evaluated by Student's *t*-test. $P < 0.01$ was considered statistically significant.

WESTERN BLOT ANALYSIS

Equal numbers (5.5×10^5 cells/6-well plates) of sub-cultured (3rd passage) normal stromal cells were allowed to attach and spread overnight, and the medium was replaced with a serum-free medium and cells were cultured for 24 h. Thereafter, cells were treated with TGF-β2 (2 ng/ml) in serum free medium, either together with SB203580 (20 μM) or SB431542 (20 μM) for 24 h. Conditioned media were collected for examine the level of secreted fibronectin, and equal volumes of supernatant (500 μl) were precipitated with a 10% ice-cold trichloroacetic acid (TCA). Precipitates were washed twice with 100% acetone to remove the remaining TCA. Air-dried precipitates were dissolved in a RIPA buffer. For cell lysates, stromal cells were extracted in RIPA buffer with protease inhibitors. Equal amounts of conditioned media or cell lysates (20 μg) were separated by 7.5% SDS–PAGE under reducing conditions, and the proteins were electrophoretically transferred to nitrocellulose membranes. Next, detection of α-SMA and fibronectin was carried out with an ECL western blotting kit according to the manufacturer's instructions.

RESULTS

TEMPORAL AND SPATIAL PATTERNS OF α-SMA IN FIBROTIC WOUND HEALING CORNEAS

In penetrating full-thickness wounds, quiescent stromal keratocytes undergo striking phenotypic changes, designated 'activation', and transform into active fibroblasts and myofibroblasts. During the contraction phase of wound healing myofibroblast appears. Myofibroblasts are characterized by the intracellular appearance of α-SMA, the most reliable marker for myofibroblasts [Tomasek et al., 2002]. To determine the temporal and spatial presence of myofibroblasts in the fibrotic healing cornea, we performed α-SMA staining. At day 1 after wounding (Fig. 1A), no α-SMA was detected in the stroma. However, at day 3 (Fig. 1B), α-SMA-expressing myofibroblasts correlating with timing of wound contraction appeared in the wound edge just underneath the repairing epithelium and within the posterior region of wound stroma. The active fibroblasts continue to differentiate over time into the

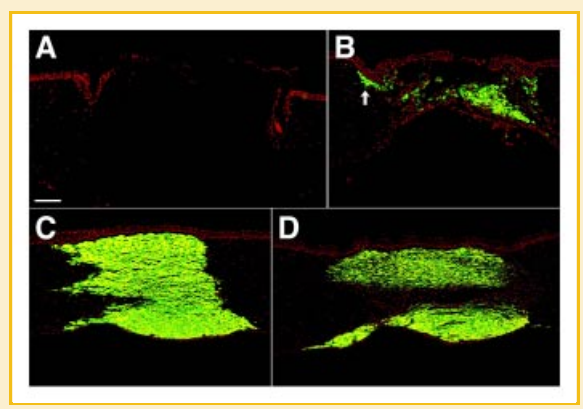

Fig. 1. Representative immunofluorescence staining for α-SMA in fibrotic healing corneas. Paraffin sections were labeled with α-SMA specific antibody and Alexa-Fluor 488-conjugated goat anti-mouse antibody (green), and cell nuclei were stained with PI (red). A: day 1 after penetrating wound. B: day 3 wound. α-SMA stain appeared in the wound edge just underneath the repairing epithelium, and within the posterior region of wound stroma. C: day 7 wound. The entire stroma was positive for α-SMA. D: day 14 wound. Intense staining was detected only in the anterior and posterior parts of healing stroma, but not the narrow region of central stroma. Confocal microscopic images are representative of at least three different experiments. Scale bars: 100 μm.

myofibroblasts. By day 7 (Fig. 1C), most (if not all) cells in the entire repairing stroma expressed α-SMA, suggesting the production of fibrotic ECM and the rate of wound contraction of healing stroma may peak about the seventh day. Thereafter, the number of myofibroblasts in healing stroma decreased at day 14. Interestingly, myofibroblasts were present mostly in the anterior and posterior repairing stroma, but were mostly absent in the narrow region of central stroma (Fig. 1D). Kitano and Goldman (1966) have described the cellular and histochemical changes in the corneal scar over time as the repair tissue matures. Our finding suggests that regression of corneal fibrosis may due to a continuous decreased numbers of myofibroblasts.

TEMPORAL AND SPATIAL PATTERNS OF LAMININ IN FIBROTIC WOUND HEALING CORNEA

The epithelium and the underlying stroma are separated by the basement membrane (BM). Intact BM displays selective permeability to the various diffusible cytokines derived from either side of the BM [Baldwin and Marshall, 2002; Stramer et al., 2003]. Upon BM disruption, epithelial cell derived cytokines such as TGF-ß are released into the stroma during corneal wound healing [Stramer et al., 2003; Gabison et al., 2009]. In normal corneas (Fig. 2A), laminin (green) was detected both in the epithelial BM and Descemet's membrane (DM). DM is a modified BM of the corneal endothelium enriched with laminin and type IV collagen [Fitch et al., 1990; Danielsen, 2004]. The reappearance of the BM after wounding was examined by indirect immunofluorescence localization of laminin. By day 3 following re-epithelialization (Fig. 2B), the BM was reconstituted with laminin just underneath the repairing epithelium. In addition, diffuse laminin staining was detected in the anterior region of the wound stroma. Negative control using day 14 repairing corneas displayed no laminin staining (Fig. 2C). By days 7 (Fig. 2D) and 14 (Fig. 2E), complete laminin staining was clearly observed along the epithelial BM. Maturation of the epithelial BM may prevent release of cytokines from the epithelium into the anterior stroma. By contrast, although large amounts of laminin were detected in the posterior region of wound stroma, there was lack of DM. Therefore, it seems likely that large amounts of TGF-β2 derived from endothelium could be released into the posterior stroma in chick (Fig. 4E). Although DM was not repaired once damaged, maintenance of endothelial integrity is paramount in fibrotic corneal wound healing in this study, as loss of endothelial cell could affect pump activities and barrier functions and result in enhanced hydration of corneas [Joyce, 2003].

TEMPORAL AND SPATIAL DISTRIBUTION OF TGF-β1, -2, AND -3 IN FIBROTIC WOUND HEALING CORNEAS

To elucidate the roles of TGF-βs during fibrotic wound healing, we analyzed the distribution of the three TGF-β isoforms at various times after creation of the penetrating wound. In normal corneas, extracellular TGF-β1 was weakly detected in BL only (Fig. 3A). In each healing cornea at day 1 (Fig. 3B), a large quantity of TGF-β1 was deposited, particularly in the anterior region of the acellular fibrin clot, a substrate for both migrating epithelium and adjacent active fibroblasts [Fini and Stramer, 2005]. By day 3 (Fig. 3C), while TGF-β1 staining was evident in the acellular region of the fibrin clot, TGF-β1 was not detected in active fibroblast/myofibroblasts within the fibrin clot. By contrast, the wound edges of a few active

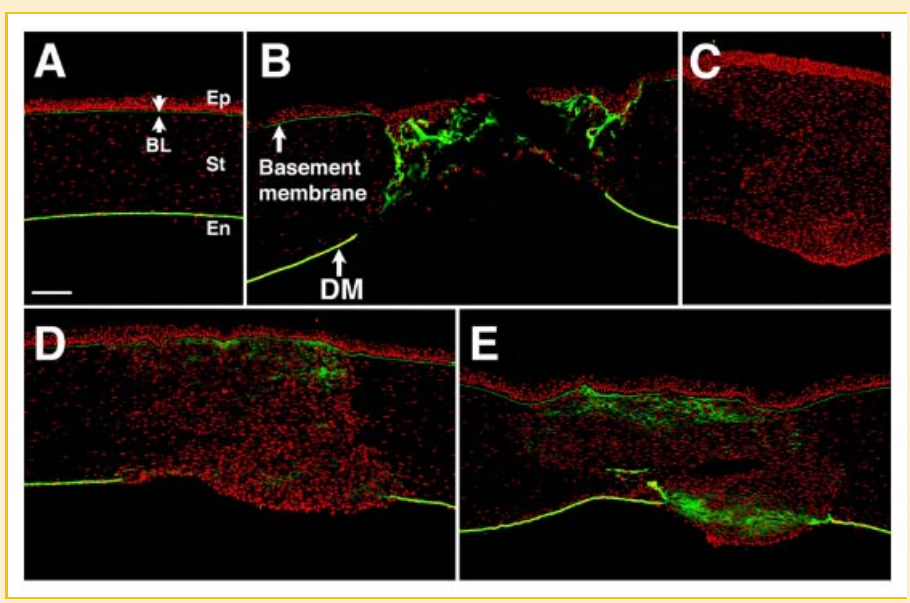

Fig. 2. Representative immunofluorescence staining for laminin in fibrotic healing corneas. Paraffin sections were labeled with laminin-specific antibody and Alexa-Fluor 488-conjugated goat anti-mouse antibody (green), and cell nuclei were stained with PI (red). A: In normal cornea, laminin staining was higher in DM (Descemet's membrane) than epithelial basement membrane (Ep, Epithelium; St, Stroma; En, Endothelium, BL, Bowman's layer). B: day 3 after wound generation, laminin appeared in the basement membrane just underneath the repairing epithelium. By days 7 (D) and 14 (E), a laminin signals were clearly present along the epithelial basement membrane and unwounded region of DM. In stroma, laminin staining was restricted to the most anterior and posterior repairing stroma. Notably, DM was not regenerated. C: Negative control at day 14 wound. Confocal microscopic images are representative of at least three different experiments. Scale bars: 100 μm.

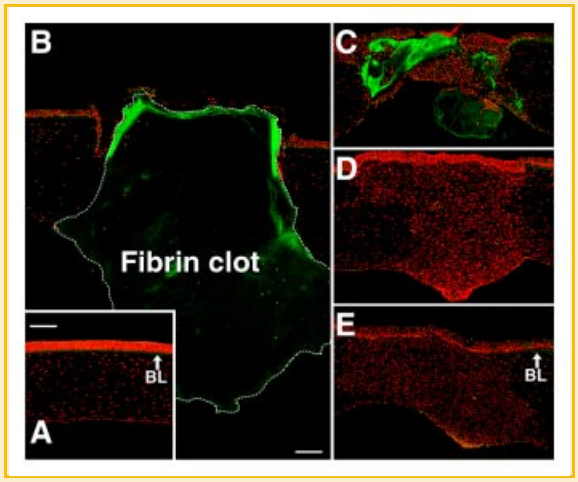

Fig. 3. Representative immunofluorescence staining of TGF-β1 in fibrotic healing corneas. Paraffin sections were labeled with TGF-β1-specific antibody and Alexa-Fluor 488-conjugated goat anti-mouse antibody (green), and cell nuclei were stained with PI (red). A: In normal cornea, TGF-β1 was weakly detected only in the Bowman's layer (BL). B: day 1 wound, TGF-β1 was deposited predominantly in the anterior region of the acellular fibrin clot (dotted line). C: day 3 wound. D: day 7 wound. E: day 14 wound. The TGF-β1 signal was clearly present throughout the healing periods in the unwounded region of BL. Confocal microscopic images are representative of at least three different experiments. Scale bars: 100 μm.

fibroblasts and endothelial cells expressed TGF-β1. Interestingly, TGF-β1 was not detected in the multi-layered epithelium that grew over the fibrin clot, but low levels were observed in the unwounded region of basal epithelial cells. By day 7 (Fig. 3D), extracellular TGF-β1 was clearly present only in the unwounded region of BL. TGF-β1 was additionally detected in occasional cells of the wounded stroma. By day 14 (Fig. 3E), TGF-β1 was detected in the wound edge of a few active fibroblasts, as well as the wound region of central endothelial cells, and unwounded region of BL. In contrast, no TGF-β1 was detected in the BL wound area, suggesting that BL is not regenerated after injury.

In normal corneas, cytoplasmic TGF-β2 was weakly detected in basal epithelial and endothelial cells (Fig. 4A). Notably, by day 1 after wounding (Fig. 4B), a TGF-β2 signal was evident in the cytoplasm of basal epithelial cells in the unwounded region. In contrast to TGF-β1 staining, the TGF-β2 signal was only faintly detected in the fibrin clot. By day 3 (Fig. 4C), a weak TGF-β2 signal was also detected in resurfacing epithelial cells within the wound region. Furthermore, numerous fibroblast/myofibroblasts populating the posterior region of the wound stroma expressed TGF-β2. By day 7 (Fig. 4D), a strong TGF-β2 signal was observed in most basal and wing cells outside the wound region, but was weakly detected in basal cells within the wound. In addition, TGF-β2 signal was evident in endothelial cells of both unwound and wound regions. Furthermore, numerous TGF-β2 expressing cells were detected especially in the anterior and posterior regions. By day 14 (Fig. 4E), a

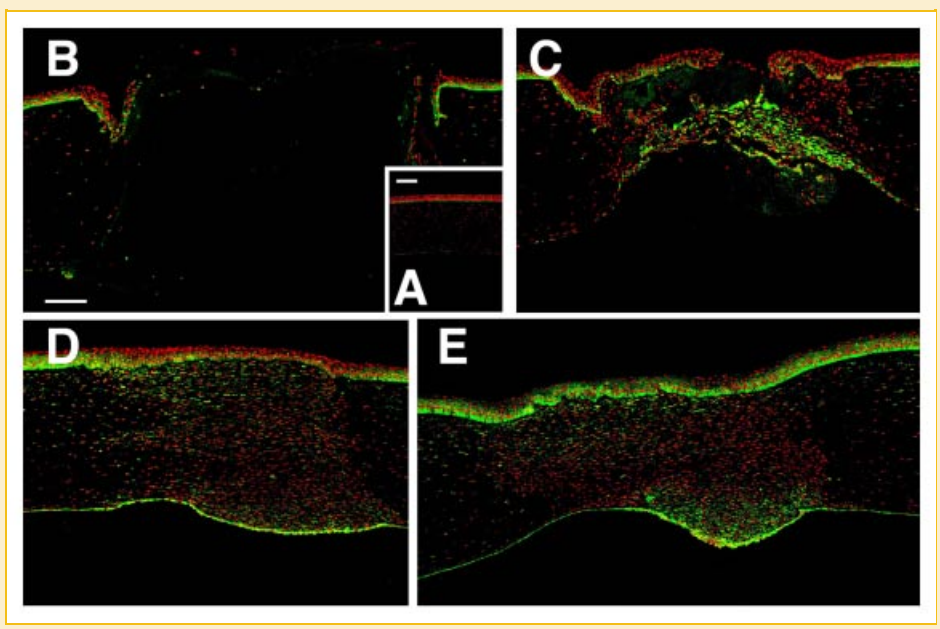

Fig. 4. Representative immunofluorescence staining of TGF-β2 in fibrotic healing corneas. Paraffin sections were labeled with TGF-β2 specific antibody and Alexa-Fluor 488-conjugated goat anti-mouse antibody (green), and cell nuclei were stained with PI (red). A: In normal cornea, cytoplasmic TGF-β2 staining was weakly detected in basal epithelial and endothelial cells. B: day 1 wound. C: day 3 wound. D: day 7 wound. A TGF-β2 signal was detected in endothelial cells, both in wounded and unwounded regions, and in the entire stromal cells. E: By day 14, its signal was detected in both wound and unwounded regions of most epithelial and endothelial cells. Numerous cells, particularly in the posterior and anterior stroma, compared to few cells in the region of central stroma expressed TGF-β2. Confocal microscopic images are representative of at least three different experiments. Scale bars: 100 μm.

TGF-β2 staining was highly detected in both the wound and normal regions of most epithelial and endothelial cells. In the healing stroma, staining patterns were similar to those at day 7. However, numerous cells, particularly posterior stroma that presumably comprise myofibroblasts, expressed TGF-β2. In contrast, few cells in the narrow region of the central stroma were positive for TGF-β2. TGF-β2 was additionally detected in the unwounded regions of many active fibroblasts. Notably, the pattern of TGF-β2 staining was similar to that of α-SMA.

In normal corneas, weak but evident cytoplasmic TGF-β3 staining was distinguished only in basal epithelial cells (Fig. 5A). At day 1 of wound generation (Fig. 5B), a TGF-β3 signal was detected in the cytoplasm of basal epithelial cells in the unwounded region. By day 3 (Fig. 5C), TGF-β3-positive staining was detected in a few epithelial cells in the wound region. In contrast, TGF-β3 was barely detectable in epithelial cells of the wound region at days 7 (Fig. 5D) and 14 (Fig. 5E). However, both basal and wing epithelial cells in the unwounded region stained for TGF-β3. Notably, TGF-β3 was absent in the healing stroma up to day 14.

TEMPORAL AND SPATIAL PATTERNS OF pSmad2 IN FIBROTIC WOUND HEALING CORNEAS

To clarify whether the Smad2 pathway is involved in fibrotic wound healing, we examined the temporal and spatial regulation of pSmad2 at various times after wounding. We employed an anti-phospho-Smad2 antibody that specifically recognizes active pSmad2 present in the nucleus, as indicated by the yellow color in the merged images. In normal corneas, pSmad2 was detected in occasional proliferating basal epithelial cells, but not in either stromal or endothelial cells (Fig. 6A). At day 1 after wound creation (Fig. 6B), nuclear pSmad2 staining (yellow) was observed in most basal epithelial cells and many active fibroblasts adjacent to the wound region. By day 3 (Fig. 6C), the active fibroblasts at wound edges, as well as the numerous fibroblast/myofibroblasts populating the posterior wound region, stained positive for nuclear pSmad2. In contrast to day 1, pSmad2 was present in only a small number of basal epithelial cells along the wound region. Many regenerating as well as unwounded endothelial cells were stained with pSmad2. By day 7 (Fig. 6E), few basal epithelial cells, but many endothelial cells, particularly in the wound region, displayed nuclear pSmad2 staining. Furthermore, numerous active fibroblasts adjacent to the wound region and in the posterior region of the healing stroma stained positive for pSmad2. By day 14 (Fig. 6F), numerous basal and wing epithelial cells along the cornea displayed pSmad2-positive staining. A pSmad2 expression was evident in the wound region of endothelial cells. In the repairing stroma, the nuclear pSmad2 signal was detected in many active fibroblasts adjacent to the wound region. Strikingly, pSmad2 staining was detected along the wound margin of fibroblasts, and some fibroblasts in the central region of the healing stroma (dotted lines: boundaries of the pSmad2 stained area). Higher magnification of asterisks regions of (C) and (F) was in (D) and (G), respectively.

TEMPORAL AND SPATIAL PATTERNS OF p38MAPK IN FIBROTIC WOUND HEALING CORNEAS

Endogenous TGF-β activates p38MAPK for epithelial cell migration and suppression of cell proliferation in an epithelial debridement wound [Saika, 2004]. However, the role of p38MAPK in fibrotic

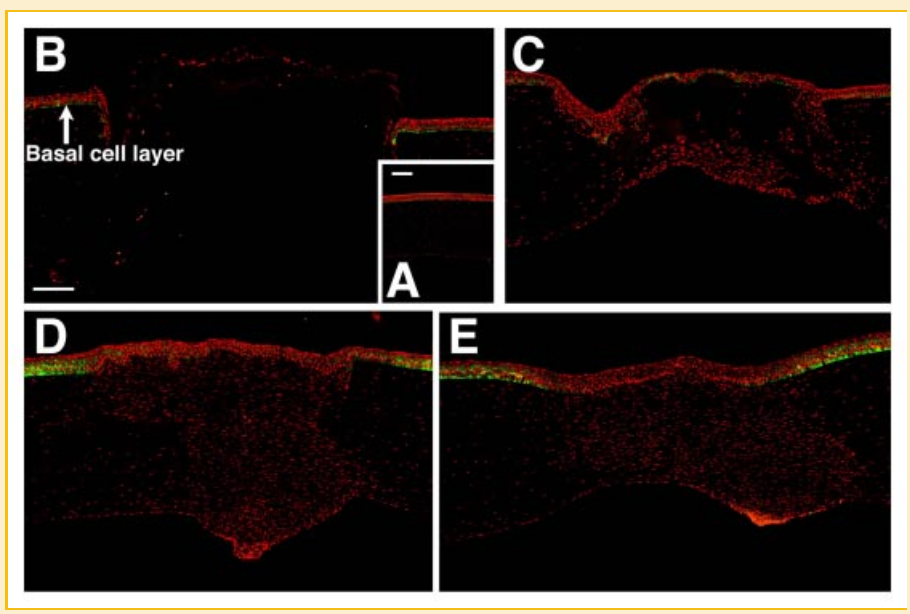

Fig. 5. Representative immunofluorescence staining of TGF-β3 in fibrotic healing corneas. Paraffin sections were labeled with TGF-β3 specific antibody and Alexa-Fluor 488-conjugated goat anti-mouse antibody (green), and cell nuclei were stained with PI (red). A: In normal cornea, cytoplasmic TGF-β3 staining was detected only in basal epithelial cells. B: day 1 wound. C: day 3 wound. By day 7 (D) and 14 (E), no protein was detected in regenerating epithelial cells in the wound region, but was expressed in both basal and wing epithelial cells in the unwounded region. Healing stroma stained negative for TGF-β3. Confocal microscopic images are representative of at least three different experiments. Scale bars: 100 μm.

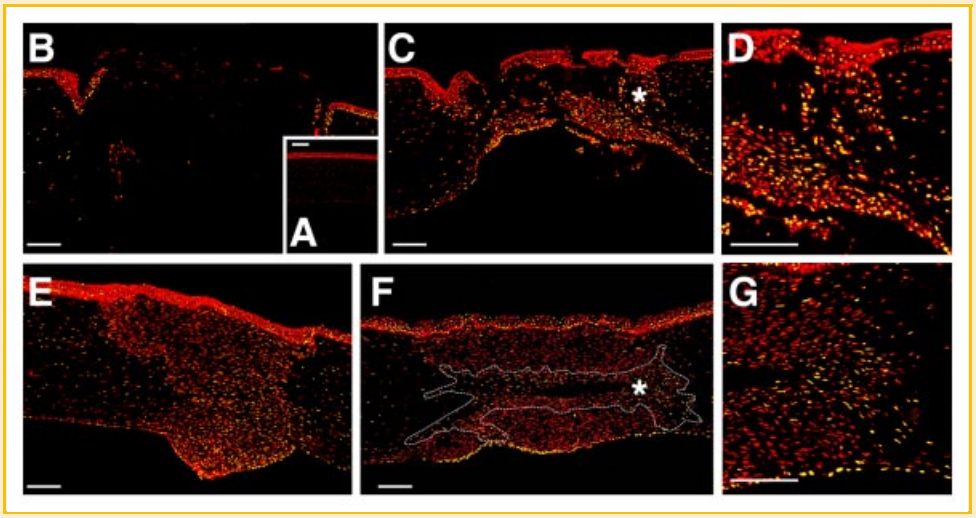

Fig. 6. Representative immunofluorescence staining of pSmad2 in fibrotic healing corneas. Paraffin sections were labeled with pSmad2 specific antibody and Alexa-Fluor 488-conjugated goat anti-mouse antibody (green), and cell nuclei were stained with PI (red). The pSmad2 signal located in the nucleus is indicated in yellow in the merged images. A: In normal cornea, pSmad2 staining was detected only in occasional proliferating basal cells. B: day 1 wound. C: day 3 wound. Its signal was detected in the active fibroblasts at wound edges, numerous cells populating the posterior wound region, few basal cells along the wound region, and regenerating endothelial cells. E: day 7 wound. Several regenerating endothelial cells and active fibroblasts/myofibroblasts, adjacent to the wound region and the posterior region of stroma, were stained with pSmad2. F: day 14 wound. In stroma, its signal was detected in active fibroblasts adjacent to the wound region, as well as along the wound margin of fibroblasts and central region of healing stroma (dotted lines: boundaries of pSmad2 stained area). Higher magnification of asterisks regions of (C) and (F) was in (D) and (G), respectively. All pSmad2 signals were nuclear (yellow). Confocal microscopic images are representative of at least three different experiments. Scale bars: 100 μm.

repairing corneas remains to be established. Accordingly, we examined the temporal and spatial staining patterns of p38MAPK in healing corneas at various times after wound generation. In normal corneas, cytoplasmic p38MAPK was detected only in occasional epithelial cells (Fig. 7A). At day 1 following wounding (Fig. 7B), a cytoplasmic p38MAPK signal was detected in most basal epithelial cells in the unwounded region. The few active fibroblasts adjacent to the wound region also stained positive for p38MAPK. By day 3 (Fig. 7C), both cytoplasmic and nuclear p38MAPK were detected in many basal and wing epithelial cells in the unwounded region. In the regenerating epithelium, weak cytoplasmic staining was observed in basal cells. In the stroma, both the cytoplasm and nuclei of many active fibroblasts near the wound region, and the mass of fibroblasts/myofibroblasts populating the posterior wound region stained positive for p38MAPK. Strikingly, a nuclear p38MAPK was detected in the wound margin of many active fibroblasts. By day 7 (Fig. 7D), the staining pattern in the epithelium was similar to that at day 3, but the signal was significantly stronger. Surprisingly, several cytoplasmic and nuclear p38MAPK-stained cells were present in the entire healing stroma and the adjacent wound region. Nuclear p38MAPK staining was also observed in the wound region of endothelial cells. By day 14 (Fig. 7E), a nuclear and cytoplasmic p38MAPK was observed in many basal and wing epithelial cells in the unwounded region. In the wound region, a higher level of cytoplasmic p38MAPK was detected in epithelial cells, but its signal was less intense than that in the wound region. Nuclear p38MAPK staining was also observed in few basal and wing epithelial cells. In stroma, the numerous anterior and posterior regions of cells displayed both nuclear and cytoplasmic p38MAPK, but staining patterns were higher in the posterior region than anterior region. Few p38MAPK-positive cells were detected in the central region (dotted lines). The pattern of p38MAPK staining was similar to those of α-SMA and TGF-β2 in the fibrotic healing corneas.

CO-LOCALIZATION OF TGF-β-2, α-SMA, AND p38MAPK IN FIBROTIC WOUND HEALING STROMAS

Immunofluorescent staining of 14-day wound corneas was performed to co-localize of p38MAPK with α-SMA (Fig. 8). Cells within the anterior and posterior part of the wound showed co-localization of p38MAPK and α-SMA within the wound, but not in the narrow region of central stroma. Furthermore, TGF-β2 staining pattern was similar to those of α-SMA and p38MAPK (Fig. 8).

α-SMA EXPRESSION THROUGH p38MAPK PATHWAYS IS MEDIATED, IN PART, BY ENDOGENOUS TGF-β-2 DURING FIBROTIC REPAIR IN CORNEAL STROMA

To examine whether blocking of p38MAPK inhibits the expression of α-SMA expression, isolated stromal cells at 14 days after wounding were subjected to primary culture. In control culture of second passages of stromal cells, α-SMA expressing myofibroblasts (42.3%) were examined by immunofluorescence (Fig. 9). SB203580 is an inhibitor of p38MAPK, while SB431542 inhibits TGF-β type I receptor kinase, the upstream activator of p38MAPK. As expected, the number of α-SMA expressing cells was greatly reduced by SB203580 or SB431542 treatment (Fig. 9A,B).

Previous report showed that TGF-β stimulated formation of stress fibers and α-SMA expression, but filamentous actin staining was reduced in stomal cells isolated from Smad3 deficient mice [Stramer et al., 2005]. In sub-cultured stromal cells (3rd passages) isolated from normal chick corneas, we found that SB431542 treatment

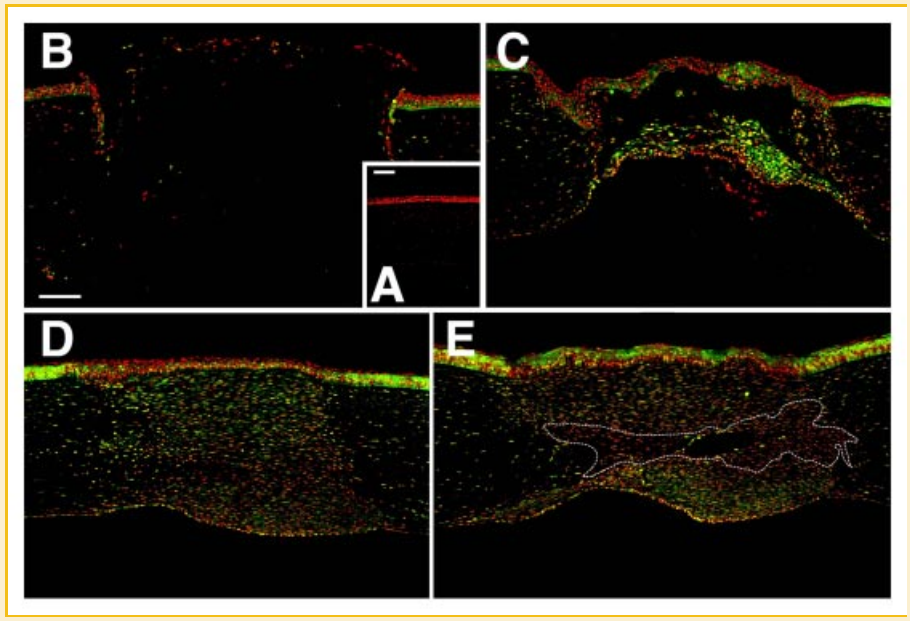

Fig. 7. Representative immunofluorescence staining of p38MAPK in fibrotic healing corneas. Paraffin sections were labeled with p38MAPK-specific antibody and Alexa-Fluor 488-conjugated goat anti-mouse antibody (green), and cell nuclei were stained with PI (red). A: In normal cornea, cytoplasmic p38MAPK staining (green) was detected in the occasional epithelial cell. B: day 1 wound. Nuclear staining (yellow) was detected in a few active fibroblasts adjacent to the wound region. C: day 3 wound. Basal and wing epithelial cells in the unwounded region displayed cytoplasmic and nuclear staining, compared to the wound region. Furthermore, the wound margin of many active fibroblasts as well as myofibroblasts populating the posterior wound region contained the protein in both cytoplasm and nucleus. D: day 7 wound. Cytoplasmic and nuclear signals were detected in cells within the entire healing stroma and adjacent to the wound region. Nuclear staining was additionally observed in the wound region of endothelial cells. E: day 14 wound. Both nucleic and cytoplasmic staining for p38MAPK was distinguished in the numerous anterior and posterior regions of cells in wound stroma. A few p38MAPK-positive cells were detected in the central region of healing stroma (dotted lines). Confocal microscopic images are representative of at least three different experiments. Scale bars: 100 μm.

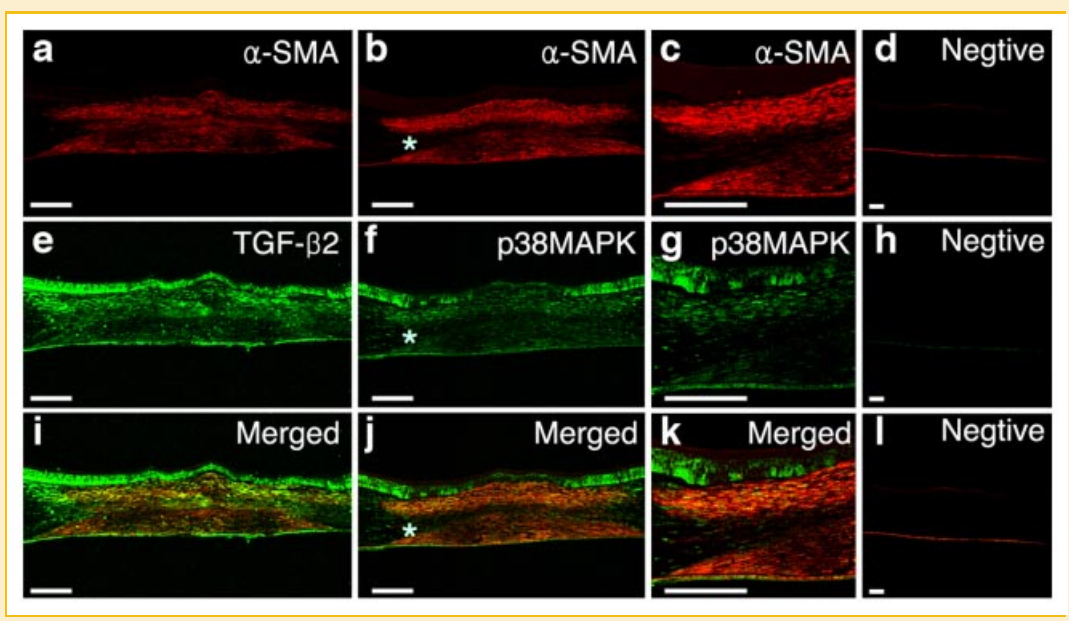

Fig. 8. Co-localization of p38MAPK and α-SMA in fibrotic healing stromas. Paraffin sections at day 14 wound were labeled with α-SMA, TGF-β2, and p38MAPK specific antibodies. Co-localization of α-SMA (b) and p38MAPK (f) was prominent in the stroma (j). Note that staining of TGF-β2 (e), α-SMA (a, b, and c) and p38MAPK (f and g) was present mostly in the anterior and posterior repairing stroma, but was mostly absent in the narrow region of central stroma. Merged image of (a) and (e) was (i). Higher magnification of asterisks regions of (b), (f), and (j) was (c), (g), and (k), respectively. Negative controls were incubated only with secondary antibodies conjugated with TRITC (red; d) and Alexa-Fluor 488 (green; h). Merged image of (d) and (h) was (l). Scale bars: 100 mm.

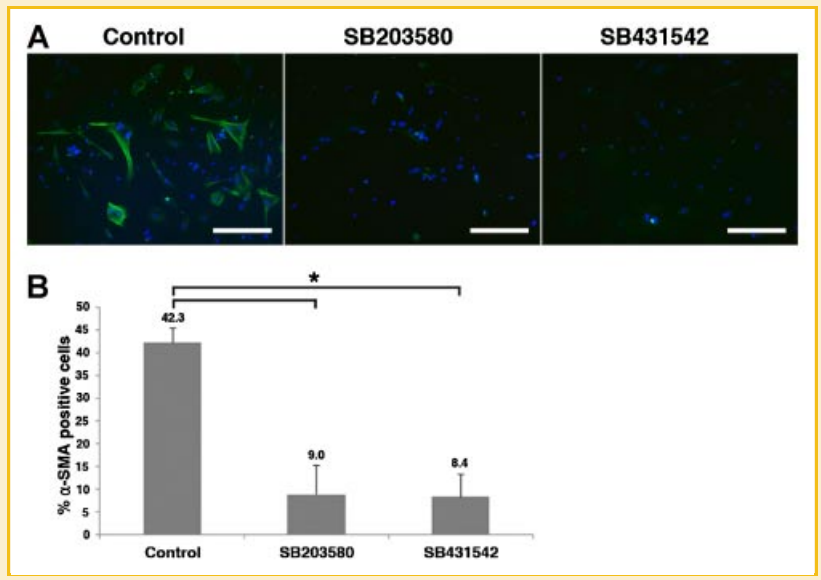

Fig. 9. Inhibition of α-SMA staining in cultured repair stromal cells by p38MAPK inhibition. Equal numbers (1.5×10^4 cells/well) of second passages of repair stromal cells isolated from healing corneas on day 14 were treated with SB203580 (20 μM) or SB431542 (20 μM) for 24 h. Compare to control culture, note that α-SMA staining (green) was significantly reduced by a p38MAPK inhibitor, SB203580 (20 μM) or a selective inhibitor of TGF-β type I receptor kinase, SB431542 (20 μM). Cell nuclei were stained with DAPI (blue). The data are means ± SE of values from four independent experiments. $^*P < 0.05$ versus corresponding value for controls. Scale bars: 50 μm.

attenuated the TGF-β2-induced α-SMA expression and formation of stress fibers. By contrast, although SB203580 decreased TGF-β2-induced α-SMA expression, formation of stress fibers was not affected (Fig. 10A,B). Compare to α-SMA expression patterns, TGF-β2-induced fibronectin secretion was greatly reduced by SB431542, but not by SB203580 (Fig. 10C). These data suggest that TGF-β2-induced myofibroblast transformation may involve a p38MAPK-dependent signal transduction pathway.

DISCUSSION

TGF-β is an important cytokine in the regulation of production and accumulation of ECM. Fibrosis is a continuous wound-healing process that results in scar formation. The structure and composition of the chick cornea is very similar to that of the human cornea, which contains a BL [Gordon et al., 1994, 1996; Sundarraj et al., 1998]. Using the chick as a model system, our present data suggest that early TGF-β signaling appears to be due to TGF-β1. Furthermore, the up-regulation of TGF-β2 of cells migrating into the stroma most likely is related to the stimulation of an autocrine TGF-β2 loop by TGF-β1.

It is well known that TGF-β2 is the major form [Imanishi et al., 2000; Maltseva et al., 2001], whereas TGF-β1 is detected in small amounts in the cornea [Wilson et al., 1994; Imanishi et al., 2000]. No TGF-β3 is present in the anterior eye [Pasquale et al., 1993; Imanishi et al., 2000]. Upon inducing a penetrating wound in each chick, the fibrin clot derived from precursors in aqueous humor was well formed in the wound area (Fig. 3), consistent with previous reports [Cintron et al., 1973, 1982; Fini and Stramer, 2005]. Acellular fibrin clot effectively sealed the hole soon after wounding and allowed the anterior chamber to re-form [Cintron et al., 1982]. Both TGF-β1 and TGF-β2 are present in human tear fluid; however, TGF-β1 is the predominant isoform [Gupta et al., 1996]. High levels of TGF-β1 in tear fluid are detected in the early days of wound healing, following photorefractive keratectomy (PRK) [Vesaluoma et al., 1997; Tuominen et al., 2001; Lee et al., 2002]. Increased TGF-β1 in tears may play an important role in scar formation in trachoma [Satici et al., 2003]. By contrast to skin and other organs, the source of TGF-β1within the fibrin clot is not derived from platelets at the wound sites of avascular cornea [Fini and Stramer, 2005]. In this study, higher levels of TGF-β1, presumably derived from tears, were present especially in the anterior region of fibrin clot within the wound region at one day after wound induction (Fig. 3B). In the intact cornea, the epithelial BM binds cytokines [Soubrane et al., 1990; Kim et al., 1999], supportive of its role as a barrier for signaling molecules from epithelium or tear fluid [Serini et al., 1998]. Although TGF-β1 is absent in unwounded or wounded epithelium in mice [Stramer et al., 2003], low-level TGF-β1 was observed at BL in normal chick cornea (Fig. 3A). Interestingly, TGF-β1 was also detected in the unwounded region of BL throughout the healing periods (Fig. 3). These differences may be species-specific. Earlier immunostaining data for Mac1, a marker of both monocytes and polymorphonuclear cells, suggest that infiltrating inflammatory cells produce and deposit TGF-β1 within the early fibrin clot [Stramer et al., 2003]. Unfortunately, we could not evaluate the role of inflammatory cells.

A number of cytokines, including IL-1α and TGF-β tend to have opposite activities, are expressed in the wound corneal epithelium and diffused into the stroma in vivo [West-Mays et al., 1997, 1999; Fini and Stramer, 2005]. TGF-β1 is involved in the regulation of keratocyte activation, myofibroblast transformation

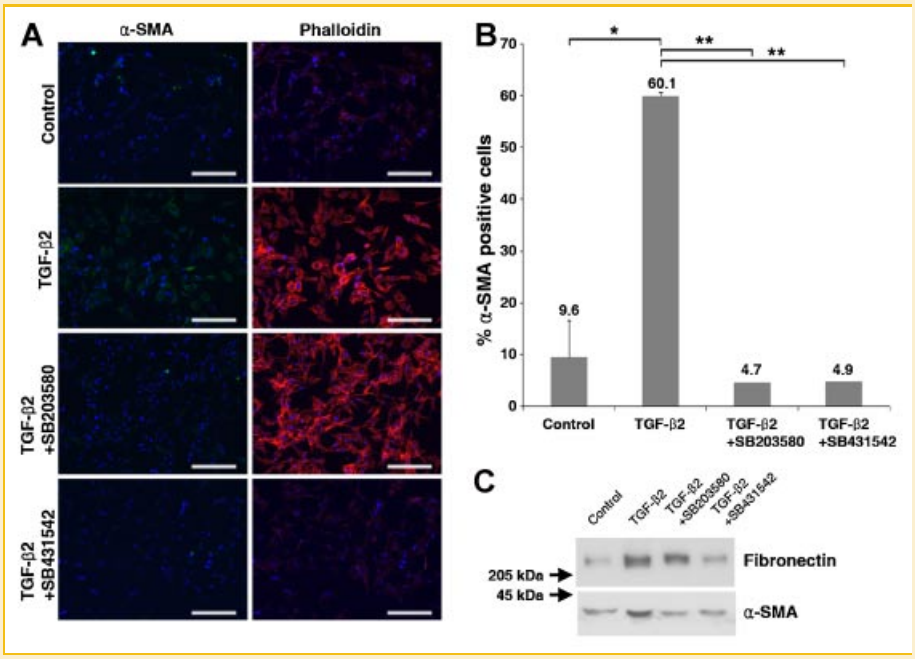

Fig. 10. Inhibition of TGF-β2-induced α-SMA expression in cultured normal stromal cells by p38MAPK inhibition. A: Equal numbers (1.5×10^4 cells/well) of sub-cultured (second passage) stromal cells isolated from normal chick corneas were serum-starved, and treated with TGF-β2 in the presence of SB203580 (20 μM) or SB431542 (20 μM) for 24 h. Direct immunofluorescence for α-SMA was performed with a primary FITC-conjugated anti-α-SMA antibody. Filamentous actin was visualized with rhodamine-conjugated phalloidin. Scale bars: 50 μm. B: Statistical analysis. TGF-β2-induced α-SMA positive cells numbers were significantly reduced by treatment with SB203580 or SB431542. The data are means ± SE of values from four independent experiments. $^{*}P < 0.05$ and $^{**}P < 0.01$ versus corresponding value for controls. C: Equal numbers (5.5×10^5 cells/6-well) of sub-cultured (third passage) stromal cells were serum-starved, and treated with TGF-β2 in the presence of SB203580 (20 μM) or SB431542 (20 μM) for 24 h. Western blot analysis of fibronectin secretion or α-SMA expression was performed using equal amounts of conditioned media or protein lysates, respectively.

and proliferation, and wound healing after refractive surgery [Jester et al., 1996; Andresen et al., 1997; Andresen and Ehlers, 1998; Moller-Pedersen et al., 1998; Beales et al., 1999]. The effects of TGF-β depend on the cell types and culture conditions, as well as the dose and characteristics of ECM [Song et al., 2000]. TGF-β1 expression is regulated by the status of the wound repair, and TGF-β1 mediates only early phases of wound repair associated with cell migration in vitro [Song et al., 2002]. In this study, epithelial cells surrounding the wound edge migrate over the anterior region of the fibrin clot, and cover the abraded region at day 3 (Fig. 3C). This step appears to be regulated by various cytokines, including TGF-β1. Surprisingly, TGF-β3 was present mainly in the epithelial cells outside the original wound area throughout healing periods (Fig. 5). Although previous studies showed that TGF-β is believed to inhibit corneal epithelial cell proliferation in vivo and in vitro [Saika et al., 2004], we found that TGF-β3 besides TGF-β1 and TGF-β2 stimulated chick corneal epithelial cell proliferation in vitro (unpublished data). Therefore, it seems likely that TGF-β3 may stimulate epithelial cell proliferation in unwound region, but not involve in the proliferation of regenerating epithelium in the central wound region. Compared to TGF-β3, TGF-β2 signal was temporally and spatially regulated and was detected in the wound region of epithelial cells (Fig. 4). Therefore, it seems likely that the activity of TGF-β2 may stimulate proliferation and stratification of regenerating epithelial cell in the central wound region. It has been shown that TGF-β activated the p38MAPK pathway, rather than the Smad pathway, and inhibited cell proliferation of migrating epithelial cells. Furthermore, inhibition of the p38MAPK pathway slowed epithelial cell migration in organ-cultured cornea after epithelial after epithelial debridement wounding [Saika, 2004]. By contrast, in our results, a similar staining pattern of TGF-β2 and p38MAPK was observed in the entire epithelial cell layer throughout healing periods (Figs. 4 and 7). These data suggest that TGF-β2-mediated p38MAPK pathway in part may modulate epithelial cell proliferation in fibrotic wound repair.

Activated keratocytes at the wound edge migrate into the fibrin clot. Initially, the acellular fibrin clot is diminished, and largely replaced by active fibroblasts that quickly become myofibroblasts (Fig. 1) synthesizing TGF-β2 (Fig. 4), but not TGF-β1 (Fig. 3). Conditioned media from myofibroblast cultures contain more active TGF-β than media from fibroblast cultures [Masur et al., 1996]. At day 3 following wound inductions, it is likely that active fibroblasts in the posterior stroma undergo a second type of transformation into myofibroblasts, mediated in part by TGF-β2. Based on the co-localized staining of α-SMA and TGF-β2 in the healing stroma at day 14 (Fig. 8), we suggest that TGF-β2 plays an important role in myofibroblast transformation in the stroma. The continuous presence of myofibroblasts is characteristic of fibrotic repair [Friedman, 1993]. Following anterior keratectomy wound, newly synthesized connective tissue containing collagen was detected in wound site and synthesis of connective tissue began after re-epithelialization of the wound surface [Tuft et al., 1989]. Likewise, stromal wound healing and remodeling gradually lead to stromal

thickening by day 7 after wounding because connective tissues were newly synthesized. In addition, α-SMA staining was evident in the whole stroma at day 7 (Fig. 1C), but disappeared in the central region at day 14 (Fig. 1D), and the fibrotic tissue appeared narrow and short. Fibrotic tissue is associated with an increment in the overall numbers of both active fibroblasts and myofibroblasts within the wound region, and maintenance of their activation status. Removal of excessive myofibroblasts may trigger a dramatic improvement in corneal function [Mathew et al., 1994]. TGF-β3 was not detectable in both epithelial and endothelial cells and in the healing stroma of the wound region (Fig. 5). Likewise, neutralizing antibodies against TGF-β1 and TGF-β2, but not TGF-β3, reduce cutaneous scarring [Shah et al., 1995]. Our findings collectively suggest that initially deposited TGF-β1 in the fibrin clot is an important factor for preliminary scar formation, and subsequent continuous remodeling of this collagenous matrix is mediated by its concerted action with TGF-β2.

TGF-β activates multiple signaling cascades, including ERK, JNK and p38MAPK and Smads [Derynck and Zhang, 2003], and is implicated in wound healing. Since Smads do have distinct roles, Samd2 and Smad3 are key signaling proteins downstream of TGF-β [Saika, 2004]. Smad3 protein has been shown to play an important role in corneal wound models in mice [Saika, 2004; Fini and Stramer, 2005; Saika et al., 2005]. Expression of α-SMA is reduced in repairing corneas of mice deficient in Smad3 [Fini and Stramer, 2005]. Although previous studies have shown that TGF-β1 induces myofibroblast transformation in vitro mediated by the Smad2 signaling pathway [Petridou et al., 2000], we found that TGF-β2 and its relationships with downstream p38MAPK signaling pathways regulate myofibroblast transformation in vitro (Fig. 10). Previously, the issue of whether activation of Smad2 or p38MAPK occurs during keratocyte transition to repair fibroblasts or myofibroblast phenotype in vivo has not been investigated. In this study, we detected high levels of TGF-β2, pSmad2 and p38MAPK in active fibroblasts at day 3 (Figs. 4, 6, and 7), suggesting that their activation is partly due to induction of TGF-β2, and both signal pathways may play an important role in the early healing period. Importantly, spatial α-SMA and p38MAPK staining patterns are well correlated at day 14 (Figs. 1, 7, and 8). In addition, the number of α-SMA expressing cells in cultured stromal cell isolated from 14 days after wounding was significantly reduced by p38MAPK inhibition (Fig. 9), suggest that the p38MAPK signaling pathway is required for the myofibroblast transformation.

In vitro cultured fibroblasts in serum under low-density culture conditions and in the presence of TGF-β1, lost cell–cell contact and transformed into myofibroblasts [Masur et al., 1996]. Furthermore, Smad2 activation in cultured fibroblasts upon TGF-β1 treatment correlated with transformation of myofibroblasts [Petridou et al., 2000]. Conditioned media from low-density cultures of myofibroblasts contain more TGF-β than high-density cultures [Masur et al., 1996]. However, cultured stromal cells in serum-free medium remain quiescent and dendritic in morphology, similar to keratocytes, and never developed a fibroblastic shape [Beales et al., 1999]. In contrast to myofibroblasts induced from passaged normal fibroblasts due to TGF-β1 treatment under low-density [Masur et al., 1996], hypercellular myofibroblasts populate the healing cornea in vivo, where they contact each other and highly express TGF-β2. Therefore, it seems likely that TGF-β2 is an important factor for myofibroblast transformation in vivo (Figs. 1, 4, and 8).

Although endothelial cells do not normally divide by multiple anti-proliferative factors and by contact inhibition between endothelial cells in vivo [Funaki et al., 2003; Joyce, 2003, 2005]. Following injury of endothelium, endothelial cells enlarge and migrate with lack of cell proliferation, but in ex vivo organ culture model, corneal endothelial cells proliferate in response to wounding [Senoo and Joyce, 2000]. Although corneal endothelial cells in vivo are arrested in G1-phase of the cell cycle, it has been suggested that peripheral region of the endothelium in vivo contains progenitor cells that could act as a source of cell renewal for the central region [Joyce, 2003; Whikehart et al., 2005]. Among anti-proliferative factors, TGF-β2, abundantly present in aqueous humor, controls the proliferation of corneal endothelial cells [Jampel et al., 1990]. Exogenous TGF-β2 or aqueous humor suppressed corneal endothelial cell proliferation [Chen et al., 1999], and significantly stimulated Smad2 phosphorylation [Funaki et al., 2003]. Moreover, adenovirus-mediated over-expression of Smad7 abolished the inhibitory effects of TGF-β2 on corneal endothelial cell proliferation that was significantly associated with suppression of Smad2 phosphorylation, and accelerated wound closure in vitro [Funaki et al., 2003]. Many growth factors besides TGF-β2 were expressed in the corneal epithelial cells, fibroblasts and endothelial cells in corneal wound healing [Wilson et al., 1992; Beales et al., 1999; Lee et al., 2002], suggesting that multiple cross-talk signal pathways or other unknown factors may additionally involve in the regulation of endothelial cell proliferation and regeneration. After injury, TGF-β2 levels in regenerating endothelium were markedly elevated at day 7 and particularly intense by day 14 after injury (Fig. 4). Based on similar expression patterns of TGF-β2 with Smad2 and p38MAPK in the endothelium (Figs. 6 and 7), our present data suggest that TGF-β2 mediated both signaling pathways may not be directly involved in regulation of endothelial cell proliferation and regeneration. In addition, once endothelial layer was regenerated, it is possible that inhibition of endothelial cell proliferation and maintenance of endothelial integrity could be regulated by constitutively expressed high levels of TGF-β2 in the endothelial cells during wound healing.

At present, there is no clear understanding of how myofibroblasts are induced in vivo during hypercellular situations in the wound region. However, it is important to highlight that TGF-β2-mediated fibroblast activation through TGF-β type I receptor kinase activity for α-SMA expression is mediated, at least partly, by the p38MAPK pathway in vivo. The issue of whether specific temporal and spatial inhibition of TGF-β2-mediated p38MAPK is required for effective prevention of fibrosis remains to be established.

REFERENCES

Andresen JL, Ehlers N. 1998. Chemotaxis of human keratocytes is increased by platelet-derived growth factor-BB, epidermal growth factor, transforming growth factor-alpha, acidic fibroblast growth factor, insulin-like growth factor-I, and transforming growth factor-beta. Curr Eye Res 17:79–87.

Andresen JL, Ledet T, Ehlers N. 1997. Keratocyte migration and peptide growth factors: The effect of PDGF, bFGF, EGF, IGF-I, aFGF and TGF-beta on human keratocyte migration in a collagen gel. Curr Eye Res 16:605–613.

Baldwin HC, Marshall J. 2002. Growth factors in corneal wound healing following refractive surgery: A review. Acta Ophthalmol Scand 80:238–247.

Barcellos-Hoff MH. 1996. Latency and activation in the control of TGF-beta. J Mammary Gland Biol Neoplasia 1:353–363.

Beales MP, Funderburgh JL, Jester JV, Hassell JR. 1999. Proteoglycan synthesis by bovine keratocytes and corneal fibroblasts: Maintenance of the keratocyte phenotype in culture. Invest Ophthalmol Vis Sci 40:1658–1663.

Cheifetz S, Hernandez H, Laiho M, ten Dijke P, Iwata KK, Massague J. 1990. Distinct transforming growth factor-beta (TGF-beta) receptor subsets as determinants of cellular responsiveness to three TGF-beta isoforms. J Biol Chem 265:20533–20538.

Chen KH, Harris DL, Joyce NC. 1999. TGF-beta2 in aqueous humor suppresses S-phase entry in cultured corneal endothelial cells. Invest Ophthalmol Vis Sci 40:2513–2519.

Cintron C, Schneider H, Kublin C. 1973. Corneal scar formation. Exp Eye Res 17:251–259.

Cintron C, Szamier RB, Hassinger LC, Kublin CL. 1982. Scanning electron microscopy of rabbit corneal scars. Invest Ophthalmol Vis Sci 23:50–63.

Danielsen CC. 2004. Tensile mechanical and creep properties of Descemet's membrane and lens capsule. Exp Eye Res 79:343–350.

Derynck R, Zhang YE. 2003. Smad-dependent and Smad-independent pathways in TGF-beta family signalling. Nature 425:577–584.

Fini ME. 1999. Keratocyte and fibroblast phenotypes in the repairing cornea. Prog Retin Eye Res 18:529–551.

Fini ME, Stramer BM. 2005. How the cornea heals: Cornea-specific repair mechanisms affecting surgical outcomes. Cornea 24:S2–S11.

Fitch JM, Birk DE, Linsenmayer C, Linsenmayer TF. 1990. The spatial organization of Descemet's membrane-associated type IV collagen in the avian cornea. J Cell Biol 110:1457–1468.

Friedman SL. 1993. Seminars in medicine of the Beth Israel Hospital, Boston. The cellular basis of hepatic fibrosis. Mechanisms and treatment strategies. N Engl J Med 328:1828–1835.

Funaki T, Nakao A, Ebihara N, Setoguchi Y, Fukuchi Y, Okumura K, Ra C, Ogawa H, Kanai A. 2003. Smad7 suppresses the inhibitory effect of TGF-beta2 on corneal endothelial cell proliferation and accelerates corneal endothelial wound closure in vitro. Cornea 22:153–159.

Gabison EE, Huet E, Baudouin C, Menashi S. 2009. Direct epithelial-stromal interaction in corneal wound healing: Role of EMMPRIN/CD147 in MMPs induction and beyond. Prog Retin Eye Res 28:19–33.

Girard MT, Matsubara M, Kublin C, Tessier MJ, Cintron C, Fini ME. 1993. Stromal fibroblasts synthesize collagenase and stromelysin during long-term tissue remodeling. J Cell Sci 104(Pt 4): 1001–1011.

Gordon MK, Foley JW, Birk DE, Fitch JM, Linsenmayer TF. 1994. Type V collagen and Bowman's membrane. Quantitation of mRNA in corneal epithelium and stroma. J Biol Chem 269:24959–24966.

Gordon MK, Foley JW, Lisenmayer TF, Fitch JM. 1996. Temporal expression of types XII and XIV collagen mRNA and protein during avian corneal development. Dev Dyn 206:49–58.

Gupta A, Monroy D, Ji Z, Yoshino K, Huang A, Pflugfelder SC. 1996. Transforming growth factor beta-1 and beta-2 in human tear fluid. Curr Eye Res 15:605–614.

Hutcheon AE, Guo XQ, Stepp MA, Simon KJ, Weinreb PH, Violette SM, Zieske JD. 2005. Effect of wound type on Smad 2 and 4 translocation. Invest Ophthalmol Vis Sci 46:2362–2368.

Imanishi J, Kamiyama K, Iguchi I, Kita M, Sotozono C, Kinoshita S. 2000. Growth factors: Importance in wound healing and maintenance of transparency of the cornea. Prog Retin Eye Res 19:113–129.

Jampel HD, Roche N, Stark WJ, Roberts AB. 1990. Transforming growth factor-beta in human aqueous humor. Curr Eye Res 9:963–969.

Jester JV, Barry-Lane PA, Cavanagh HD, Petroll WM. 1996. Induction of alpha-smooth muscle actin expression and myofibroblast transformation in cultured corneal keratocytes. Cornea 15:505–516.

Joyce NC. 2003. Proliferative capacity of the corneal endothelium. Prog Retin Eye Res 22:359–389.

Joyce NC. 2005. Cell cycle status in human corneal endothelium. Exp Eye Res 81:629–638.

Jung JC, Huh MI, Fini ME. 2007. Constitutive collagenase-1 synthesis through MAPK pathways is mediated, in part, by endogenous IL-1alpha during fibrotic repair in corneal stroma. J Cell Biochem 102:453–462.

Kim WJ, Mohan RR, Mohan RR, Wilson SE. 1999. Effect of PDGF, IL-1alpha, and BMP2/4 on corneal fibroblast chemotaxis: Expression of the platelet-derived growth factor system in the cornea. Invest Ophthalmol Vis Sci 40:1364–1372.

Kitano S, Goldman JN. 1966. Cytologic and histochemical changes in corneal wound repair. Arch Ophthalmol 76:345–354.

Koli K, Saharinen J, Hyytiainen M, Penttinen C, Keski-Oja J. 2001. Latency, activation, and binding proteins of TGF-beta. Microsc Res Tech 52:354–362.

Lee JB, Choe CM, Kim HS, Seo KY, Seong GJ, Kim EK. 2002. Comparison of TGF-beta1 in tears following laser subepithelial keratomileusis and photorefractive keratectomy. J Refract Surg 18:130–134.

Maltseva O, Folger P, Zekaria D, Petridou S, Masur SK. 2001. Fibroblast growth factor reversal of the corneal myofibroblast phenotype. Invest Ophthalmol Vis Sci 42:2490–2495.

Massague J. 2003. Integration of Smad and MAPK pathways: A link and a linker revisited. Genes Dev 17:2993–2997.

Masur SK, Dewal HS, Dinh TT, Erenburg I, Petridou S. 1996. Myofibroblasts differentiate from fibroblasts when plated at low density. Proc Natl Acad Sci USA 93:4219–4223.

Mathew J, Hines JE, James OF, Burt AD. 1994. Non-parenchymal cell responses in paracetamol (acetaminophen)-induced liver injury. J Hepatol 20:537–541.

Moller-Pedersen T, Cavanagh HD, Petroll WM, Jester JV. 1998. Neutralizing antibody to TGFbeta modulates stromal fibrosis but not regression of photoablative effect following PRK. Curr Eye Res 17:736–747.

Myers JS, Gomes JA, Siepser SB, Rapuano CJ, Eagle RC, Jr., Thom SB. 1997. Effect of transforming growth factor beta 1 on stromal haze following excimer laser photorefractive keratectomy in rabbits. J Refract Surg 13:356–361.

Nomura M, Li E. 1998. Smad2 role in mesoderm formation, left-right patterning and craniofacial development. Nature 393:786–790.

Pasquale LR, Dorman-Pease ME, Lutty GA, Quigley HA, Jampel HD. 1993. Immunolocalization of TGF-beta 1, TGF-beta 2, and TGF-beta 3 in the anterior segment of the human eye. Invest Ophthalmol Vis Sci 34:23–30.

Petridou S, Maltseva O, Spanakis S, Masur SK. 2000. TGF-beta receptor expression and smad2 localization are cell density dependent in fibroblasts. Invest Ophthalmol Vis Sci 41:89–95.

Piek E, Ju WJ, Heyer J, Escalante-Alcalde D, Stewart CL, Weinstein M, Deng C, Kucherlapati R, Bottinger EP, Roberts AB. 2001. Functional characterization of transforming growth factor beta signaling in Smad2- and Smad3-deficient fibroblasts. J Biol Chem 276:19945–19953.

Saika S. 2004. TGF-beta signal transduction in corneal wound healing as a therapeutic target. Cornea 23:S25–S30.

Saika S, Okada Y, Miyamoto T, Yamanaka O, Ohnishi Y, Ooshima A, Liu CY, Weng D, Kao WW. 2004. Role of p38 MAP kinase in regulation of cell

migration and proliferation in healing corneal epithelium. Invest Ophthalmol Vis Sci 45:100–109.

Saika S, Ikeda K, Yamanaka O, Miyamoto T, Ohnishi Y, Sato M, Muragaki Y, Ooshima A, Nakajima Y, Kao WW, Flanders KC, Roberts AB. 2005. Expression of Smad7 in mouse eyes accelerates healing of corneal tissue after exposure to alkali. Am J Pathol 166:1405–1418.

Satici A, Guzey M, Dogan Z, Kilic A. 2003. Relationship between Tear TNF-alpha, TGF-beta1, and EGF levels and severity of conjunctival cicatrization in patients with inactive trachoma. Ophthalmic Res 35:301–305.

Senoo T, Joyce NC. 2000. Cell cycle kinetics in corneal endothelium from old and young donors. Invest Ophthalmol Vis Sci 41:660–667.

Serini G, Bochaton-Piallat ML, Ropraz P, Geinoz A, Borsi L, Zardi L, Gabbiani G. 1998. The fibronectin domain ED-A is crucial for myofibroblastic phenotype induction by transforming growth factor-beta1. J Cell Biol 142:873–881.

Shah M, Foreman DM, Ferguson MW. 1995. Neutralisation of TGF-beta 1 and TGF-beta 2 or exogenous addition of TGF-beta 3 to cutaneous rat wounds reduces scarring. J Cell Sci 108(Pt 3): 985–1002.

Sharma GD, He J, Bazan HE. 2003. p38 and ERK1/2 coordinate cellular migration and proliferation in epithelial wound healing: Evidence of cross-talk activation between MAP kinase cascades. J Biol Chem 278:21989–21997.

Song QH, Singh RP, Richardson TP, Nugent MA, Trinkaus-Randall V. 2000. Transforming growth factor-beta1 expression in cultured corneal fibroblasts in response to injury. J Cell Biochem 77:186–199.

Song QH, Klepeis VE, Nugent MA, Trinkaus-Randall V. 2002. TGF-beta1 regulates TGF-beta1 and FGF-2 mRNA expression during fibroblast wound healing. Mol Pathol 55:164–176.

Soubrane G, Jerdan J, Karpouzas I, Fayein NA, Glaser B, Coscas G, Courtois Y, Jeanny JC. 1990. Binding of basic fibroblast growth factor to normal and neovascularized rabbit cornea. Invest Ophthalmol Vis Sci 31:323–333.

Stramer BM, Zieske JD, Jung JC, Austin JS, Fini ME. 2003. Molecular mechanisms controlling the fibrotic repair phenotype in cornea: Implications for surgical outcomes. Invest Ophthalmol Vis Sci 44:4237–4246.

Stramer BM, Austin JS, Roberts AB, Fini ME. 2005. Selective reduction of fibrotic markers in repairing corneas of mice deficient in Smad3. J Cell Physiol 203:226–232.

Sundarraj N, Fite D, Belak R, Sundarraj S, Rada J, Okamoto S, Hassell J. 1998. Proteoglycan distribution during healing of corneal stromal wounds in chick. Exp Eye Res 67:433–442.

Tomasek JJ, Gabbiani G, Hinz B, Chaponnier C, Brown RA. 2002. Myofibroblasts and mechano-regulation of connective tissue remodelling. Nat Rev Mol Cell Biol 3:349–363.

Tsukada S, Westwick JK, Ikejima K, Sato N, Rippe RA. 2005. SMAD and p38 MAPK signaling pathways independently regulate alpha1(I) collagen gene expression in unstimulated and transforming growth factor-beta-stimulated hepatic stellate cells. J Biol Chem 280:10055–10064.

Tuft SJ, Zabel RW, Marshall J. 1989. Corneal repair following keratectomy. A comparison between conventional surgery and laser photoablation. Invest Ophthalmol Vis Sci 30:1769–1777.

Tuominen IS, Tervo TM, Teppo AM, Valle TU, Gronhagen-Riska C, Vesaluoma MH. 2001. Human tear fluid PDGF-BB, TNF-alpha and TGF-beta1 vs corneal haze and regeneration of corneal epithelium and subbasal nerve plexus after PRK. Exp Eye Res 72:631–641.

Vesaluoma M, Teppo AM, Gronhagen-Riska C, Tervo T. 1997. Release of TGF-beta 1 and VEGF in tears following photorefractive keratectomy. Curr Eye Res 16:19–25.

Weinstein M, Yang X, Li C, Xu X, Gotay J, Deng CX. 1998. Failure of egg cylinder elongation and mesoderm induction in mouse embryos lacking the tumor suppressor smad2. Proc Natl Acad Sci USA 95:9378–9383.

West-Mays JA, Sadow PM, Tobin TW, Strissel KJ, Cintron C, Fini ME. 1997. Repair phenotype in corneal fibroblasts is controlled by an interleukin-1 alpha autocrine feedback loop. Invest Ophthalmol Vis Sci 38:1367–1379.

West-Mays JA, Cook JR, Sadow PM, Mullady DK, Bargagna-Mohan P, Strissel KJ, Fini ME. 1999. Differential inhibition of collagenase and interleukin-1alpha gene expression in cultured corneal fibroblasts by TGF-beta, dexamethasone, and retinoic acid. Invest Ophthalmol Vis Sci 40:887–896.

Whikehart DR, Parikh CH, Vaughn AV, Mishler K, Edelhauser HF. 2005. Evidence suggesting the existence of stem cells for the human corneal endothelium. Mol Vis 11:816–824.

Wilson SE, He YG, Lloyd SA. 1992. EGF, EGF receptor, basic FGF, TGF beta-1, and IL-1 alpha mRNA in human corneal epithelial cells and stromal fibroblasts. Invest Ophthalmol Vis Sci 33:1756–1765.

Wilson SE, Schultz GS, Chegini N, Weng J, He YG. 1994. Epidermal growth factor, transforming growth factor alpha, transforming growth factor beta, acidic fibroblast growth factor, basic fibroblast growth factor, and interleukin-1 proteins in the cornea. Exp Eye Res 59:63–71.